Hydrogen Diffusion and Trapping in α-Iron: The Role of Quantum and Anharmonic Fluctuations

Bingqing Cheng,[1] Anthony T. Paxton,[2] and Michele Ceriotti[1]
[1]*Laboratory of Computational Science and Modeling, Institute of Materials, École Polytechnique Fédérale de Lausanne, 1015 Lausanne, Switzerland*
[2]*Department of Physics, King's College London. Strand, London WC2R 2LS, United Kingdom*

(Received 23 February 2018; revised manuscript received 9 April 2018; published 31 May 2018)

We investigate the thermodynamics and kinetics of a hydrogen interstitial in magnetic α-iron, taking account of the quantum fluctuations of the proton as well as the anharmonicities of lattice vibrations and hydrogen hopping. We show that the diffusivity of hydrogen in the lattice of bcc iron deviates strongly from an Arrhenius behavior at and below room temperature. We compare a quantum transition state theory to explicit ring polymer molecular dynamics in the calculation of diffusivity. We then address the trapping of hydrogen by a vacancy as a prototype lattice defect. By a sequence of steps in a thought experiment, each involving a thermodynamic integration, we are able to separate out the binding free energy of a proton to a defect into harmonic and anharmonic, and classical and quantum contributions. We find that about 30% of a typical binding free energy of hydrogen to a lattice defect in iron is accounted for by finite temperature effects, and about half of these arise from quantum proton fluctuations. This has huge implications for the comparison between thermal desorption and permeation experiments and standard electronic structure theory. The implications are even greater for the interpretation of muon spin resonance experiments.

DOI: 10.1103/PhysRevLett.120.225901

The injection, transport, and trapping of subatomic particles such as protons, deuterons, tritons, muons, or positrons in solids takes a pivotal role in experimental characterization techniques such as muon spin rotation spectroscopy (μSR) [1], positron annihilation experiments [2,3], and in the design of plasma containment in fusion power generators [4]. In the case of hydrogen, diffusion and trapping is also crucial in many technological and materials science applications, including, for instance, hydrogen storage and fuel cells [5,6], in particular the deleterious effects of hydrogen on electrode integrity as a consequence of the Gorski effect. Diffusion of hydrogen in iron is also of interest in the final stages of stellar evolution [7]. The problem of hydrogen embrittlement of iron and steel is deeply connected with the rate of proton diffusion and the depth of lattice defect traps that may serve to attenuate the diffusivity, since it is expected that the crack tip speed may be limited by the rate at which it can be fed by hydrogen [8]. The trapping of hydrogen by vacancies is of particular importance because by the defactant effect [9], the vacancy is stabilized by trapping, and indeed, the equilibrium vacancy concentration is known to be enhanced by orders of magnitude as a result of hydrogen ingress [10], leading to damage and a compromised structural integrity [11]. The depth of a microstructural trap—that is, the free energy gain by transferring a proton from a bulk tetrahedral site into the trap—is extremely hard to measure, since although an average trap depth over many defects is accessible through thermal desorption spectroscopy, it is not possible to prepare specimens with just a single defect in order to distinguish, say, a dislocation trap from a grain boundary or interface site. This is particularly difficult in the case of the vacancy. It is possible to calculate trap depths using density functional theory (DFT), and for example, it has been shown that the vacancy may trap up to five protons—one close to each face of the cube surrounding the defect [12]. Unfortunately, standard DFT calculations have ready access only to the zero temperature total energy. The quantum nature of the subatomic particle is usually neglected or accounted for only in terms of a *post hoc* zero point energy (ZPE) correction.

Our aim in the present Letter is to unravel various contributions to the binding free energy to provide both a framework for the general case and to address the trapping of H in ferrite (α-Fe) quantitatively. Atomistic modelling of a hydrogen interstitial in α-iron poses enormous challenges. First, the magnetism requires an explicit treatment of the electronic degrees of freedom of the system [12–14]; second, the time scale required to measure the H binding free energy to defects, as well as the diffusivity in the bulk lattice, is usually not accessible in *ab initio* MD simulations. To make the matter even more complex, the small mass of the proton means that nuclear quantum effects (NQEs) can play an important role at room temperature and below. For instance, it has been demonstrated that NQEs have a significant effect on the thermodynamic stability of different phases [15–17], as well as on the diffusivity of protons [18–20].

In the present Letter, interatomic forces are described within the self-consistent magnetic tight binding (TB) approximation [21]. Parameters for the model are given in Ref. [22]. TB theory is an abstraction of the DFT, and hence, it has the benefit of capturing the essential physics of the chemical bond, including self-consistent charge transfer, with forces derived from the Hellmann-Feynman theorem. However, the method is computationally very fast because the Hamiltonian is obtained from a fitted look-up table rather than determined *ab initio*. The evaluation of NQEs is achieved by using the imaginary time path integral formalism of quantum mechanics. The path integral formalism maps the quantum mechanical partition function onto the partition function of a classical ring-polymer system [23–26], and as such, the quantum system can be described by P copies of the physical system with corresponding particles in adjacent replicas connected by harmonic springs. When $P = 1$, the nuclei are purely classical, and when $P \to \infty$, each nucleus in the ring polymer is fully consistent with the statistics of a quantum system of distinguishable particles. Methods inspired by path integral molecular dynamics (PIMD) [27,28] can also be used to approximate time-dependent observables. We will use the thermostatted ring polymer molecular dynamics (TRPMD) method [29]. The reader is referred to recent reviews for a more thorough discussion of PIMD-related methods [30,31].

In order to compute the quantum configurational distribution and the diffusivity of H in the α-Fe lattice, we first performed TRPMD simulations of a system consisting of 16 Fe atoms on a perfect bcc iron lattice, and a H interstitial atom. We performed simulations at 300, 200, 150, 100, and 50 K, increasing the number of beads P for both H and Fe atoms from 16 to 64 as the temperature was lowered, to account for the stronger quantum nature of nuclei at lower temperature. For the sake of comparison, we also performed classical simulations (i.e., only using one bead for the ring polymer) from 1000 K to 100 K. The diffusion coefficients of H in α-Fe were computed from the $\omega \to 0$ limit of the velocity-velocity autocorrelation spectrum of the H atom. Results for these simulations are reported in Fig. 1, compared with the results from a previous calculation using a classical embedded atom potential (EAM) for interatomic forces [32], as well as experimental measurements [33,34] in the high-temperature regime.

The most prominent observation from Fig. 1 is the stark difference between the classical and the quantum diffusion coefficient of H at temperatures equal or lower than room temperature. Using classical molecular dynamics, the temperature dependence closely follows Arrhenius behavior as indicated by the dashed red line. Furthermore, the classical diffusivities predicted by the TB Hamiltonian and the EAM force field are very similar. However, when nuclear quantum effects are included, either by using the path integral formalism or by employing centroid

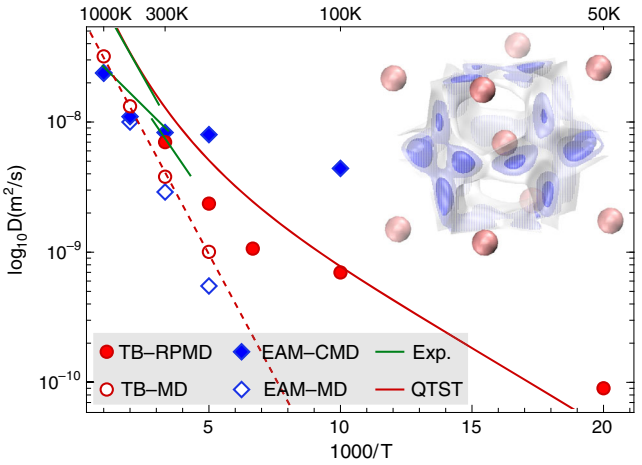

FIG. 1. Measured and calculated diffusivity of hydrogen in α-Fe. Experimental data are drawn as solid green Arrhenius lines in the temperature range of the measurements [33,34]. Blue squares are from centroid molecular dynamics simulations by Kimizuka *et al.* [32] using an embedded atom classical potential (EAM) and a Morse potential for hydrogen and iron; MD is classical molecular dynamics and CMD is centroid MD. The red curve is the result of a quantum transition state theory (QTST) calculation by Katzarov and Paxton [35,36]. The open and solid red squares are our results using the TB Hamiltonian and classical MD and path integral MD (RPMD), respectively. On the inset, the distribution of quantum mechanical H atoms in the bcc unit cell that was computed from RPMD simulations is shown.

molecular dynamics, a strong deviation of the H diffusivity from Arrhenius behavior below room temperature emerges. Notice also that the effective activation barriers of diffusion from different experiments, which determine the slopes of the green lines in Fig. 1, are different from each other and from the theoretical predictions, even though the diffusion coefficients agree well. As suggested in Ref. [37], this is because Arrhenius behavior was assumed when interpreting experimental measurements. At the low-T end of the experimental temperature range (300 K), classical MD predictions for both TB and EAM are about a factor of two lower than experiments, while quantum results for both models are in good agreement. The discrepancy between classical and quantum dynamics indicates the importance of NQEs, which become dramatic at lower temperatures (50 K to 200 K).

While the EAM and TB are in agreement in the classical MD, there is a large discrepancy at low T between the EAM-CMD and the TB-RPMD. It is not unusual to see larger discrepancies between potential energy surfaces when simulations are performed that include nuclear quantum fluctuations, because configurations explore regions that display large levels of anharmonicities, that are often not included in the fitting of the potential [38,39]. It is possible that while the EAM is fitted to the classical activation barrier, the EAM does not describe well the three-dimensional potential energy surface for H moving

around the Fe lattice. On the other hand, the TB reproduces this "adiabatic surface" in comparison to density functional calculations very well, particularly near the saddle point [40]. This means that, as the beads wander far from the classical reaction coordinate, the proton samples regions of the configuration space that the EAM does not describe well.

From the point of view of the description of quantum nuclear effects on diffusion, RPMD makes no harmonic or frozen lattice approximation, and it has been shown to describe deep-tunneling contributions to rates in a way that can be related to instanton theory [41]. It therefore provides an instructive comparison for various transition state theory approximation schemes [36,37], polaron models [42], and methods for computing tunneling integrals [43]. The quantum TST (QTST) uses fixed potential energy surfaces at the reactant basin and at the saddle point. After that, the partition functions are calculated, which means that the rate coefficient can be found without great effort at any temperature [36]. Because the rather artificial construction is made in Ref. [36] that the potential energy in configuration space is calculated using a relaxed atomic system with the proton constrained at the saddle point, the QTST would be expected to overestimate the diffusivity. On the other hand, the QTST neglects dynamic phonon effects such as phonon assisted tunneling in the polaron picture [44]. From that point of view, one might expect that the TB-RPMD would predict a greater diffusivity than the TB-QTST. As seen in Fig. 1, the opposite is the case at temperatures between 100 and 300 K. This observation suggests that in this system, phonon assisted tunneling is not a large effect, or that other effects that are included in RPMD and not in QTST and attenuate proton diffusion, such as dynamical recrossing and phonon scattering, are dominant. The qualitative agreement between TB-QTST and TB-RPMD at all temperatures validates the use of the much cheaper QTST to estimate rate coefficients in the quantum regime.

To elucidate the mechanism of H diffusion in α-Fe, we show the quantum mechanical density distribution of H at 300 K in a bcc unit cell in the inset of Fig. 1. It can be seen that the equilibrium positions for H in the lattice are tetrahedral (T) sites. Meanwhile, NQEs broaden the spread of the distribution of H around the energy minima, which indicates strong ZPE effects in the H hopping. In other words, NQEs delocalize H in the reactant state, and effectively reduce the free energy barrier for H migration between neighboring T sites.

Diffusion in the perfect bcc lattice is a necessary component of the mechanistic understanding of the mobility of H in α-Fe. However, the rate-limiting step for macroscopic diffusion always involves binding to crystal defects. In order to assess the importance of different terms in the overall binding free energy between the H atom and the defect, in the second part of our study we consider the archetypical example of a vacancy in α-Fe. Computing this binding energy by sampling of the NVT ensemble is difficult, as the waiting time for a trapped H to be released is far beyond the time scale of standard molecular dynamics. Furthermore, a very large simulation would be needed to bring the H atom sufficiently far from the vacancy to estimate accurately the binding energy in the dilute limit.

For these reasons, we decided to compute the stability of a H atom bound to a vacancy, relative to that of a H atom in a tetrahedral site of the perfect bcc lattice, by computing first the absolute Helmholtz free energies for four systems separately [45]: (i) a perfect bulk α-Fe system that has 16 atoms (Fe_{16}), (ii) a system with a vacancy (Fe_{15}), (iii) a system with a H interstitial ($Fe_{16}H$), and (iv) a system with a vacancy and a H interstitial ($Fe_{15}H$). Based on the Helmholtz free energy of the four independent systems, at a certain thermodynamic condition the binding energy of a proton to a monovacancy can be schematically expressed as $A_{V-H} = A(Fe_{16}H) + A(Fe_{15}) - A(Fe_{15}H) - A(Fe_{16})$.

To compute A for the four systems, we used the thermodynamic integration (TI) method, that uses a series of simulations of real or artificial systems to compute the various components of the free energy difference between a harmonic reference system and the fully anharmonic, quantum system. To do so efficiently, we have carefully selected a combination of multiple thermodynamic integration routes as depicted schematically in Fig. 2. This combination thus takes into account vibrational entropy, anharmonicity, and NQEs, and it makes it possible to disentangle the different contributions. Since a detailed description of thermodynamic integration routes and several tricks of the trade can be found in Ref. [46], here we only summarize the routes employed in the present Letter. The first TI route (the green arrow in Fig. 2) goes from the

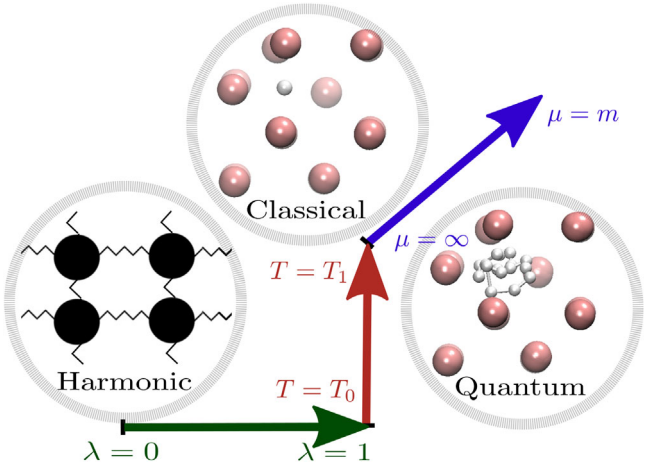

FIG. 2. Schematics of thermodynamic integration (TI) routes used in the free energy evaluations. The green arrow indicates the switching between the harmonic reference system ($\lambda = 0$) and a real system ($\lambda = 1$), the red arrow illustrates TI with respect to temperature, and the blue arrow shows TI from a classical to a quantum mechanical system.

classical harmonic crystal whose free energy A_h is analytic, to the classical physical system at $T_0 = 10$ K, At these low temperatures, the H interstitial atom does not jump between degenerate trap sites inside the vacancy during the MD simulations. The second TI route (the red arrow) allows us to obtain the temperature dependence of the Helmholtz free energies of each Fe-H system, by running simulations of the classical physical system under the *NVT* ensemble from the low temperature T_0 to a higher temperature $T_1 = 300$ K. The last TI takes into account NQEs at $T_1 = 300$ K. The overall NQEs in free energy can be evaluated from the integration of the quantum centroid virial kinetic energy with respect to the fictitious "atomic" mass μ [17,47]. In practice, the integrand was evaluated for the actual system and for systems with all the atomic masses scaled 4 and 16 times in PIMD simulations.

In Fig. 3, we plot the predictions from the harmonic approximations, the classical anharmonic free energy contribution, and the overall free energy of binding taking into account fully both anharmonicity and NQEs. Our results show that, at all temperatures, vibrational entropy plays an important role in the hydrogen-vacancy binding energy of the classical Fe-H systems as demonstrated by the considerable difference between the 0 K prediction (the black line in Fig. 3) and the classical harmonic approximation (the blue line in Fig. 3). This difference in the vibration frequencies of the vacancy-trapped and the free H in the T sites also translates to the large zero point energy

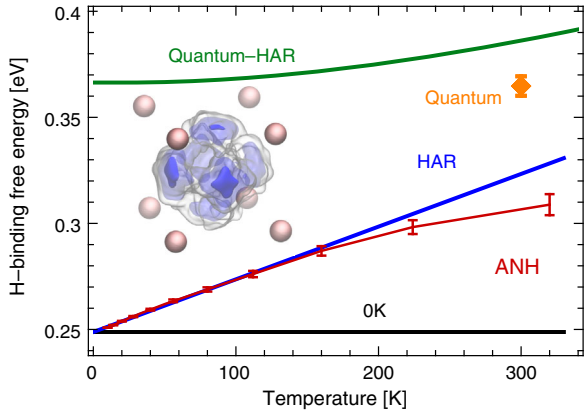

FIG. 3. The temperature dependent H binding free energy to a monovacancy in α-Fe. The black line is the prediction just using the minima of the potential energy surface at 0 K, the blue line shows the harmonic approximation for the classical system, the green line illustrate the harmonic approximation for the quantum mechanical system, the red curve indicates the fully anharmonic result of the classical system, and the yellow dot shows the quantum and anharmonic result. Statistical uncertainties are indicated by the error bars. In the inset: the distribution of quantum mechanical H atoms near a vacancy, as computed by TRPMD at 300 K. The proton spends no time at the vacant site itself; this is consistent with DFT calculations [12] and validates our TB Hamiltonian.

contribution to the overall binding free energy. This is reflected in the remarkable gap between the harmonic approximations using the classical Boltzmann distribution and the quantum mechanical Bose-Einstein distribution (the blue line and the green line in Fig. 3, respectively). Finally, anharmonicity, which has been neglected in previous DFT calculations [12,13,48–51], lowers the binding energy by about 20 meV even at room temperature. Overall, the anharmonic quantum mechanical trapping energy of H in α-Fe at 300 K is predicted to be 0.365 ± 0.005 eV. This value is lower than observed values of 0.55–0.81 eV for hydrogen trapping energy in alpha-iron [52,53], and 0.48–0.63 eV for deuterium at room temperature [54,55]. Part of the disagreement might be due to a corresponding underestimation of the baseline 0 K binding energy obtained by TB (0.25 eV) in comparison to the equivalent quantity (uncorrected for ZPE) using gradient corrected local spin density approximation, 0.45 eV [56]. On the other hand, the ZPE (0.12 eV) and the potential energy barrier (0.09 eV) predicted by the TB Hamiltonian are in an excellent agreement with DFT values [14,56], which can be seen as a proxy to quantum effects and an indicator of anharmonicity, respectively.

The magnitude of quantum and anharmonic effects, which is on a par with the difference between using different potential energy surfaces such as TB and DFT, has implications for the identification of trap sites by comparison of thermal desorption spectra and total energy calculations. In this case, ZPE would suffice to obtain a quantitative prediction of the stability of the bound state, but of course, this might not be the case for a different system or at higher temperatures. The TB Hamiltonian used in our study can be seen as an extremely attractive, indeed the only, feasible solution to take into account the quantum mechanical and anharmonic fluctuations.

In conclusion, we have characterized the importance of NQEs and anharmonicity in two of the microscopic mechanisms that underlie the transport of H atoms in α-Fe, namely H diffusion in the perfect bcc lattice, and the binding of H to a monovacancy. Nuclear quantum effects change the diffusion coefficient of H in bulk α-Fe by a factor of two at room temperature, and the quantum effects become overwhelming at lower temperatures. We then consider the case of the binding free energy of H to a monovacancy, for which we considered and disentangled different contributions such as vibrational entropy, anharmonicity, and NQEs, concluding that they all play a significant role at room temperature, and collectively increase the binding energy from 0.25 meV to 0.36 meV. This latter is closer to the experimental estimates, and the magnitude of the quantum contribution is consistent with the experimental observation that deuterium is less strongly bound than ^{1}H. Our findings thus suggest that nuclear quantum effects may have significant effects on the interactions between H atoms and other defects, which are essential in achieving a quantitative

predictive capability of the hydrogen embrittlement process. In addition, hopping and trapping of other charged subatomic particles in metal lattices is of central importance in solid state physics, encompassing phenomena such as μSR and positron annihilation experiments. There is no doubt, in view of our findings, that quantum fluctuations will take a greater part in the physics of these processes, and this study has furnished us with a recipe for how to address these questions, such as the diffusivity of a positron in a metal or semiconductor or the trap depth of a muon at a crystal defect.

M. C. and B. C. acknowledge financial support by the Swiss National Science Foundation (Project ID 200021-159896) and allocation of CPU time under the CSCS Project ID s787. A. T. P. acknowledges the support of the UK EPSRC under the Programme Grant HEmS, EP/L014742.

[1] E. Brandt and A. Seeger, Adv. Phys. **35**, 189 (1986).
[2] A. Seeger, Appl. Phys. **4**, 183 (1974).
[3] J. Slotte, I. Makkonen, and F. Tuomisto, ECS J. Solid State Sci. and Technol. **5**, 3166 (2016).
[4] R. A. Causey and T. J. Venhaus, Phys. Scr. **T94**, 9 (2001).
[5] P. L. Cabot, E. Guezala, J. C. Calpe, M. T. Garca, and J. Casado, J. Electrochem. Soc. **147**, 43 (2000).
[6] D. Alique, D. Martinez-Diaz, R. Sanz, and J. Calles, Membranes **8**, 5 (2018).
[7] E. Salpeter and H. van Horn, Astrophys. J. **155**, 183 (1969).
[8] O. Barrera, D. Bombac, Y. Chen, T. D. Daff, E. Galindo-Nava, P. Gong, D. Haley, R. Horton, I. Katzarov, J. R. Kermode, C. Liverani, M. Stopher, and F. Sweeney, J. Mater. Sci. **53**, 6251 (2018).
[9] R. Kirchheim, Acta Mater. **55**, 5129 (2007).
[10] Y. Fukai, *The Metal–Hydrogen System* (Springer-Verlag, Berlin, Heidelberg, 2005), 2nd ed.
[11] K. Takai, H. Shoda, H. Suzuki, and M. Nagumo, Acta Mater. **56**, 5158 (2008).
[12] Y. Tateyama and T. Ohno, Phys. Rev. B **67**, 174105 (2003).
[13] W. Counts, C. Wolverton, and R. Gibala, Acta Mater. **58**, 4730 (2010).
[14] A. T. Paxton, Mater. Sci. Technol. **30**, 1063 (2014).
[15] M. A. Morales, J. M. McMahon, C. Pierleoni, and D. M. Ceperley, Phys. Rev. Lett. **110**, 065702 (2013).
[16] E. A. Engel, B. Monserrat, and R. J. Needs, Phys. Rev. X **5**, 021033 (2015).
[17] M. Rossi, P. Gasparotto, and M. Ceriotti, Phys. Rev. Lett. **117**, 115702 (2016).
[18] H. Kimizuka, H. Mori, and S. Ogata, Phys. Rev. B **83**, 094110 (2011).
[19] A. Hassanali, F. Giberti, J. Cuny, T. D. Kühne, and M. Parrinello, Proc. Natl. Acad. Sci. U.S.A. **110**, 13723 (2013).
[20] M. Rossi, M. Ceriotti, and D. E. Manolopoulos, J. Phys. Chem. Lett. **7**, 3001 (2016).
[21] A. T. Paxton and M. W. Finnis, Phys. Rev. B **77**, 024428 (2008).
[22] A. T. Paxton and C. Elsässer, Phys. Rev. B **87**, 224110 (2013).
[23] R. P. Feynman and A. R. Hibbs, *Quantum Mechanics and Path Integrals* (McGraw-Hill, New York, 1964).
[24] D. Chandler and P. G. Wolynes, J. Chem. Phys. **74**, 4078 (1981).
[25] M. Parrinello and A. Rahman, J. Chem. Phys. **80**, 860 (1984).
[26] M. Ceriotti, M. Parrinello, T. E. Markland, and D. E. Manolopoulos, J. Chem. Phys. **133**, 124104 (2010).
[27] J. Cao and G. A. Voth, J. Chem. Phys. **101**, 6168 (1994).
[28] I. R. Craig and D. E. Manolopoulos, J. Chem. Phys. **121**, 3368 (2004).
[29] M. Rossi, M. Ceriotti, and D. E. Manolopoulos, J. Chem. Phys. **140**, 234116 (2014).
[30] S. Habershon, D. E. Manolopoulos, T. E. Markland, and T. F. Miller, Annu. Rev. Phys. Chem. **64**, 387 (2013).
[31] T. E. Markland and M. Ceriotti, Nat. Rev. Chem. **2**, 0109 (2018).
[32] H. Kimizuka, H. Mori, and S. Ogata, Phys. Rev. B **83**, 094110 (2011).
[33] M. Nagano, Y. Hayashi, N. Ohtani, M. Isshiki, and K. Igaki, Scr. Metall. **16**, 973 (1982).
[34] K. Kiuchi and R. B. McLellan, Acta Metall. **31**, 961 (1983).
[35] I. H. Katzarov and A. T. Paxton, in *Proceedings of the 2nd International Conference on Steel and Hydrogen*, edited by L. Duprez (OCAS, Ghent, 2014), p. F01.
[36] A. T. Paxton and I. H. Katzarov, Acta Mater. **103**, 71 (2016).
[37] D. Di Stefano, M. Mrovec, and C. Elsässer, Phys. Rev. B **92**, 224301 (2015).
[38] L. Malerba, M. Marinica, N. Anento, C. Bjrkas, H. Nguyen, C. Domain, F. Djurabekova, P. Olsson, K. Nordlund, A. Serra, D. Terentyev, F. Willaime, and C. Becquart, J. Nucl. Mater. **406**, 19 (2010).
[39] L. Wang, M. Ceriotti, and T. E. Markland, J. Chem. Phys. **141**, 104502 (2014).
[40] A. T. Paxton and C. Elsässer, Phys. Rev. B **82**, 235125 (2010).
[41] J. O. Richardson and S. C. Althorpe, J. Chem. Phys. **131**, 214106 (2009).
[42] D. Emin, M. I. Baskes, and W. D. Wilson, Phys. Rev. Lett. **42**, 791 (1979).
[43] A. Klamt and H. Teichler, Phys. Stat. Sol. (b) **134**, 533 (1986).
[44] C. P. Flynn and A. M. Stoneham, Phys. Rev. B **3**, 2819 (1971).
[45] In our experience, while surprising, a 16 atom unit cell is fully adequate for capturing the diffusion and trapping of H in α-Fe. This has been confirmed in a DFT study [56]. This is evidenced by our quantitative agreement in the diffusivity both from experiment and in comparison with published EAM findings that have the same activation energy and that use much larger supercells [32]. The ability to use the small unit cell is a considerable benefit since the number of force evaluations required for determining the diffusion coefficient and the trapping energy of H in the Fe systems is on the order of 10^7, which is beyond the capability of *ab initio* molecular dynamics.
[46] B. Cheng and M. Ceriotti, Phys. Rev. B **97**, 054102 (2018).
[47] W. Fang, J. Chen, M. Rossi, Y. Feng, X.-Z. Li, and A. Michaelides, J. Phys. Chem. Lett. **7**, 2125 (2016).

[48] O. Y. Vekilova, D. I. Bazhanov, S. I. Simak, and I. A. Abrikosov, Phys. Rev. B **80**, 024101 (2009).
[49] G. Lu and E. Kaxiras, Phys. Rev. Lett. **94**, 155501 (2005).
[50] D. F. Johnson and E. A. Carter, J. Mater. Res. **25**, 315 (2010).
[51] K. Ohsawa, K. Eguchi, H. Watanabe, M. Yamaguchi, and M. Yagi, Phys. Rev. B **85**, 094102 (2012).
[52] K.-T. Kim, S.-I. Pyun, and E. M. Riecke, J. Mater. Sci. Lett. **4**, 624 (1985).
[53] H. K. D. H. Bhadeshia, ISIJ International (1989-) (Iron and Steel Institute of Japan) **56**, 24 (2016).
[54] S. Myers, S. Picraux, and R. Stoltz, J. Appl. Phys. **50**, 5710 (1979).
[55] F. Besenbacher, S. Myers, P. Nordlander, and J. Nørskov, J. Appl. Phys. **61**, 1788 (1987).
[56] E. Hayward and C.-C. Fu, Phys. Rev. B **87**, 174103 (2013).